Journal of Applied Analysis and Computation
Volume 15, Number 6, December 2025, 3805–3825
Website:http://www.jaac-online.com
DOI:10.11948/20250039

INNOVATIVE SOLUTIONS FOR FRACTIONAL WHITHAM-BROER-KAUP MODEL USING TRANSFORM-BASED METHODS*

Azzh Saad Alshehry[1], Saima Noor[2,3,†], Abdulkafi Mohammed Saeed[4], Ahmad Shafee[5] and Rasool Shah[6,†]

Abstract This study investigates the application of the Elzaki Residual Power Series Method (ERPSM) and the New Iteration Transform Method (NITM) for solving fractional-order Whitham-Broer-Kaup system. These nonlinear fractional differential equations are fundamental models for describing complex wave dynamics and fluid mechanics phenomena. Using the fractional derivative by the proposed methods provides robust and efficient approaches for deriving analytical solutions regarding power series and other functional forms. The convergence and reliability of the methods are thoroughly analyzed, highlighting their ability to handle the intricate dynamics of fractional-order systems. Numerical simulations and illustrative examples validate the accuracy and effectiveness of ERPSM and NITM in solving fractional-order Whitham-Broer-Kaup system. The findings demonstrate the potential of these methods to address a wide range of problems in mathematical physics, fluid dynamics, and nonlinear wave theory, offering new insights into fractional-order modeling.

Keywords Elzaki residual power series method, new iteration transform method, fractional-order Whitham-Broer-Kaup system.

MSC(2010) 33B15, 34A34, 35A20, 35A22, 44A10.

[†]The corresponding authors.
[1]Department of Mathematical Sciences, Faculty of Sciences, Princess Nourah Bint Abdulrahman University, P.O. Box 84428, Riyadh 11671, Saudi Arabia
[2]Department of Basic Sciences, General Administration of Preparatory Year, King Faisal University, P.O. Box 400, 31982, Al Ahsa, Saudi Arabia
[3]Department of Mathematics and Statistics, College of Science, King Faisal University, P.O. Box 400, 31982, Al Ahsa, Saudi Arabia
[4]Department of Mathematics, College of Science, Qassim University, Buraydah 51452, Saudi Arabia
[5]PAAET, College of Technological Studies, Laboratory Technology Department, Shuwaikh 70654, Kuwait
[6]Department of Mathematics, Abdul Wali Khan University Mardan, Pakistan
*This work was supported by the Deanship of Scientific Research, Vice Presidency for Graduate Studies and Scientific Research, King Faisal University, Saudi Arabia (Grant No. KFU252477). Princess Nourah bint Abdulrahman University Researchers Supporting Project number (PNURSP2025R183), Princess Nourah bint Abdulrahman University, Riyadh, Saudi Arabia.
Email: asalshihry@pnu.edu.sa(A. S. Alshehry),
snoor@kfu.edu.sa(S. Noor), abdulkafiahmed@qu.edu.sa(A. Saeed),
as.zada@paaet.edu.kw(A. Shafee), rasoolshahawkum@gmail.com(R. Shah)

1. Introduction

Fractional calculus is the study of classical derivatives and integrals extended or generalized to non-integer order instances, and it has received a great deal of scholarly interest in the past several decades. The study of Fractional derivatives can be found in various technical and physical systems, including viscoelasticity, groundwater, the propagation of waves, finances, and fluid mechanics [6, 7, 14, 62]. Several researchers have examined theoretical outcomes derived from fractional differential equation solutions and their uniqueness in different formats; some examples of these investigations are [12, 16, 17, 19, 32, 43, 55]. Many fractional differential problems are either without closed form solutions or have too complex an analytical solution to be useful. Because of this, numerous authors have developed various numerical approximation techniques. These include the Fourier spectral methods, Finite difference schemes, the homotopy analysis approach, He's variational iteration method, Adomian's decomposition, and many others categorized in [7]. For comprehensive research on the solution of fractional differential equations, we direct our readers to the classic books and papers [6, 7]. Wang et al. [53] also offer a novel physical-constrained decomposition of thermography infrared with the better analysis of heat flux. Yang et al. [56] consider the subspace of the biquaternion windowed linear canonical transform, which has important implication in signal processing. Shi et al. [49] suggest the use of hypergraphs based model to improve the study of multi-agent Q-learning dynamics under the conditions of the public goods games. In the meantime Shi, Wang, and Yang [50] explore the small parameters analysis of Maxwell-Schrodinger systems providing an insight on advanced differential equations. Additionally, the review was conducted to explain Huang et al. [30] developments of an unconditionally stable Chebyshev finite-difference time-domain approach and Liu et al. [34] studies of the image transformation methods to identify partial discharge sources in high-speed trains. Also, Chen and Jing [18] introduce a super resolution method to video enhancement through deformable 3D convolution, and Guo et al. [27] augment RotaBaxter theory of algebra, which helps build non-abelian algebra structures.

The Broer-Kaup equation system is one of the key mathematical frameworks used to comprehend and interpret nonlinear mathematical phenomena in applied mathematics and physics. This system has a collection of quite challenging and sophisticated terminology and a community of nonlinear partial differential equations. This method is also beneficial and essential for deciphering and comprehending wave interactions and other challenging and intricate fundamental scientific processes. The primary characteristics of the Broer-Kaup system of equations are its thorough comprehension and its capacity for solution analysis and interpretation. This system offers a valuable method for grasping and interpreting intricate physical phenomena. Additionally, it has numerous applications in various domains, including fluid motion, engineering, plasma physics, and multidisciplinary fields. Learning and comprehending the Broer-Kaup system of equations presents a challenging intellectual exercise. Scholars, since it necessitates a profound comprehension of nonlinear interactions and their diverse applications [9, 40, 48, 54].

An analytical technique called the RPS approach was put out by [4] to ascertain the coefficients of a class of DEs' power series solutions. The basic idea lies in solving several linear and nonlinear equations using power series methods without linearity or perturbation. Additionally, the method calls for computing a derivative for the residual function at each step of the coefficient-finding process. Additionally, the method calls for finding the residual function's derivative at each step of the coefficient-finding process [8, 20, 39, 45, 52]. The technique in question was first introduced by Eriqat et al. [22], and its benefits stem from the fact that it requires fewer computing resources to extract the form of solutions in a power series of values defined by a series of algebraic procedures [33, 35, 61]. The proposed method leverages the idea of limits at infinity to accomplish its primary objective, even though the RPS technique does not require the idea of the derivative to be used to determine the parameters of the series's solution. Actual Accurate have been produced for several types of nonlinear and linear DEs using the LRPS technique. The suggested method is unique in that it can handle nonlinear equations, which is not possible with typical LT-based methods. The LRPS approach has recently been modified to address a variety of fractional DE problems, such as hyperbolic systems of Caputo-time-fractional PDEs with changing coefficients [5], nonlinear time-fractional dispersive PDEs [2], fuzzy Quadratic Riccati DEs [37], time-fractional nonlinear water wave PDEs [2], time-fractional Navier-Stokes equations [63], and Lane-Emden equations [36], the logistic system and Fisher's models [23], as well as nonlinear fractional reaction-diffusion for bacteria growth models [41] and so on [58–60].

Daftardar-Gejji and Jafari [26] introduced the novel iterative technique (NIM) in 2006, and it has since become an efficient mathematical tool for solving both linear and nonlinear functional equations. NIM's effectiveness is demonstrated by the numerous nonlinear problems it has been used to solve, including algebraic equations, integral equations, and ordinary or partial differential equations of both fractional and integer order. The unique features of NIM include its ease of use and comprehension, which make it available to a broad range of scholars and practitioners [10, 11, 38, 47, 57]. Compared to established techniques such as the homotopy perturbation method [28], the ADM [1], and the VIM [29], NIM has shown improved performance and better efficiency. That's why people dealing with complex nonlinear situations find it popular [24].

2. Basic definitions

This section briefly introduces the Elzaki transform and the Caputo fractional concept.

Definition 2.1. [13] The fractional operator of order $\delta \geq 0$, the Reimann-Lioville is described as

$$G^{\delta} f(\vartheta) = \begin{cases} \dfrac{1}{\Gamma(\delta)} \displaystyle\int_0^{\vartheta} \dfrac{f(s)}{(\vartheta - s)^{1-\delta}} ds = \dfrac{1}{\Gamma(\delta)} \tau^{\delta} - 1 * f(\tau), & \delta > 0, \tau > 0, \\ f(\sigma), & \delta = 0. \end{cases} \tag{2.1}$$

The convolution product of $\tau^{\delta-1}$ and $f(\tau)$ is denoted as $\tau^{\delta-1} * f(\tau)$.
The fractional integral of Riemann-Liouville can be found here.

1. $G^{\delta} \tau^{\delta} = \dfrac{\Gamma(\chi+1)}{\Gamma(\chi+\delta+1)} \tau^{\delta+\chi}, \chi > -1,$
2. $G^{\delta}(\lambda f(\tau) + \mu g(\tau)) = \lambda G^{\delta} f(\tau) + \mu G^{\delta} g(\tau).$

The real constants λ and μ are used.

Definition 2.2. [31, 44] Given a function $f(\tau) : [0, +\infty) \to R$, and m represent the $\delta(\delta > 0)$ represent the upper positive integer. The definition of the derivative of Caputo fractional is given as

$$D^{\delta} f(\tau) = \frac{1}{\Gamma(m-\tau)} \int_0^{\sigma} \frac{f^{(m)}(s)}{(\tau - s)^{(\delta+1-m)}} ds, \ m-1 < \delta \leq m, \quad m \in N. \tag{2.2}$$

Regarding the derivative of Caputo, we obtain

1. $D^{\delta} G^{\delta} f(\tau) = f(\tau)$,
2. $G^{\delta} D^{\delta} f(\tau) = f(\tau) - \sum_{i=o}^{m-1} y^{(i)}(0) \frac{\tau^i}{i!}$,
3. $D^{\delta} \tau^{\beta} = \begin{cases} \frac{\Gamma(\chi+1)}{\Gamma(\chi+1-\delta)} \tau^{\chi-\delta}, & \chi \geq \delta, \\ 0, & \chi < \delta, \end{cases}$
4. $D^{\delta} c = 0$,
5. $D^{\delta}(\lambda f(\tau) + \mu g(\tau)) = \lambda D^{\alpha} f(\tau) + \mu D^{\alpha} g(\tau)$,

with c, δ, and μ being real constants.

Definition 2.3. [3] The form of the power series is given as

$$\begin{aligned} \sum_{k=0}^{\infty} f_k(\vartheta)(\tau - \tau_0)^{k\delta} =& f_0(\vartheta) + f_1(\vartheta)(\tau - \tau_0)^{\delta} + f_2(\tau - \tau_0)^{2\delta} + \cdots, \\ & 0 < m-1 < \alpha \leq m, \quad \tau \geq \tau_0, \end{aligned} \tag{2.3}$$

regarding $\tau = \tau_0$, is referred to as multiple fractional power series. When f_k are functions of ϑ and τ is a variable are known as the series coefficients.

Theorem 2.1. *Assume that the series of numerous fractional powers represents $\varphi(\vartheta, \tau)$ at $\tau = \tau_0$ is of the following form*

$$\begin{aligned} \varphi(\vartheta, \tau) = \sum_{n=0}^{\infty} \varphi_{n(\vartheta,\tau)} = \sum_{n=0}^{\infty} f_n(\vartheta)(\tau - \tau_0)^{m\delta}, \\ 0 < m-1 < \delta \leq m, \quad \vartheta \in I, \quad \tau_o \leq \tau < \tau_0 + R, \end{aligned} \tag{2.4}$$

if $D_{\tau}^{n\delta} \varphi(\vartheta, \tau)$ are continuous on $I \times (\tau_0, \tau_0 + R), m = 0, 1, 2, \cdots$, then coefficients $f_n(\vartheta)$ of Eq. (2.4) *are of the form as*

$$f_n(\vartheta) = \frac{D_{\tau}^{n\delta} \varphi(\vartheta, \tau_o)}{\Gamma(n\delta + 1)}, \quad n = 0, 1, 2, \cdots, \tag{2.5}$$

where $D_t^{m\alpha} = \frac{\partial^{m\alpha}}{\partial t^{m\alpha}} = \frac{\partial^{\alpha}}{\partial t^{\alpha}} \cdot \frac{\partial^{\delta}}{\partial t^{\delta}} \cdots \frac{\partial^{\delta}}{\partial t^{\delta}}$ (n-times), and $R = min_{c \in I} R_c$, where the fractional power series' radius of convergence is indicated R_c by $\sum_{n=0}^{\infty} f_n(c)(\tau - \tau_0)^{n\delta}$.

The standard residual power series method's convergence indicates that there exists a real number $\lambda \in (0, 1)$, such that

$$\| \varphi_n(\vartheta, \tau) \| \leq \lambda \| \varphi_{n-1}(\vartheta, \tau) \|, \tau \in (\tau_0, \tau_0 + R).$$

Definition 2.4. [21, 51] We examine functions in the set B defined by using a novel transform termed the ELzaki transform, designed for functions of exponential order:

$$B = f(\tau) : \exists M, k_1, k_2 > 0, \quad | f(\tau) |< M \exp^{\frac{|\tau|}{k_j}}, \quad \text{if } \tau \in (-1)^j \times [0, \infty). \tag{2.6}$$

The constant must havebe a finite number for each function in the set, where k_1, k_2 may be infinite or finite. The integral equation defines the Elzaki transform

$$E[f(\tau)] = T(\nu) = \nu \int_0^{\infty} f(\tau) \exp^{\frac{-\tau}{\nu}} d\tau, \quad \tau{\geq}0, \quad k_1{\leq}\ \nu \leq k_2. \tag{2.7}$$

The definition and simple calculations get the following results

1. $E[\tau^m] = m!\nu^{n+2}$,
2. $E\left(f'\tau\right) = \dfrac{T\nu}{\nu} - \nu(f(0))$,
3. $E\left(f''\tau\right) = \dfrac{T\nu}{\nu^2} - \nu f'(0) - f(0)$,
4. $E\left(f^m\tau\right) = \dfrac{T\nu}{\nu^m} - \left(\displaystyle\sum_{k=0}^{m-1} \nu^{k-n+2}\right)\left(f^{(k)}(0)\right)$,
5. $E[\tau^\delta] = \displaystyle\int_0^\infty e^{-\tau\nu}\tau^\delta dt = \nu^{(\delta+1)}\Gamma(\delta+1), \mathbb{R}(\delta) > 0.$

Theorem 2.2. [46] *The following Elzaki transform of the derivative of Riemann-Liouville can be considered if $T(\nu)$ is the Elzaki transform of (τ)*

$$E\left[D^\delta(f(\tau)\right] = \nu^{-\delta}\Big[T(\nu) - \sum_{k=1}^{m} \nu^{\delta-k+2}[D^{\delta-k}(f(0))]\Big], \ -1 < m-1 \leq \delta < m. \tag{2.8}$$

Definition 2.5. [46] Using Theorem 2.2, an Elzaki transform associated with the Caputo fractional can be expressed as below.

$$E\left[D^\delta(f(\tau)\right] = \nu^{-\delta}E[f(\tau)] - \sum_{k=1}^{n-1} \nu^{2-\delta+k} f^{(k)}(0), \tag{2.9}$$

where $n-1 < \delta < n$.

This section provides stages and definitions for a nonlinear inhomogeneous partial differential equation and establishes its general form. The template is given as

$$D_\tau^\delta \varphi(\vartheta,\rho,\tau) = \mathcal{L}(\varphi(\vartheta,\rho,\tau)) + \mathcal{N}(\varphi(\vartheta,\rho,\tau)) + \tau(\varphi(\vartheta,\rho,\tau)) \tag{2.10}$$

with

$$\varphi_i(\vartheta,\rho,\tau) \mid_{\sigma=0}= g_k, k = 0, \cdots m-1, \tag{2.11}$$

where the general nonlinear fraction differential operator is $\mathcal{N}$, the known function is τ, and the linear fraction differential operator is $\mathcal{L}$.

For the ERPSM, we recommend the following procedures:

Step 1. When both sides of the equation are transformed using the Elzaki method, the form is

$$E[D_\tau^\delta \varphi(\vartheta,\rho,\tau)] = E[\mathcal{L}(\varphi(\vartheta,\rho,\tau)) + \mathcal{N}(\varphi(\vartheta,\rho,\tau)) + \upsilon(\varphi(\vartheta,\rho,\tau))]. \tag{2.12}$$

With the above initial conditions and the differentiation property of the Elzaki transform, we can get

$$E[D_\tau^\delta \varphi(\vartheta,\rho,\tau)] = g(\vartheta,\rho,\tau)+\nu^\delta E[\mathcal{L}(\varphi(\vartheta,\rho,\tau))+\mathcal{N}\varphi(\vartheta,\rho,\tau)+\upsilon(\varphi(\vartheta,\rho,\tau))]. \tag{2.13}$$

Step 2. Utilizing the inverse of Elzaki on both sides of the equation

$$\varphi(\vartheta,\rho,\tau) = G(\vartheta,\rho,\tau) + E^{-1}[\nu^\delta E[\mathcal{L}(\varphi(\vartheta,\rho,\tau)) + \mathcal{N}\varphi(\vartheta,\rho,\tau)) + \tau(\varphi(\vartheta,\rho,\tau))]]. \tag{2.14}$$

$G(\vartheta;\rho;\tau)$ denotes the initial condition in this case.

Step 3. Our preferred method is the classic RPSM, which can be suggested by

$$\varphi(\vartheta,\rho,\tau) = \sum_{m=0}^{\infty} f_m(\vartheta,\rho)\frac{\tau^{m\delta}}{\Gamma(1+m\delta)}. \tag{2.15}$$

To derive the approximate value of (2.15), $\varphi i(\vartheta,\rho,\tau)$ can be expressed as

$$S_i = \sum_{m=0}^{i} \varphi_m(\vartheta,\rho,\tau) = \sum_{m=0}^{\infty} f_m(\vartheta,\rho)\frac{\tau^{m\delta}}{\Gamma(1+m\delta)}. \tag{2.16}$$

Step 4. When Steps 2 and 3 are combined, we can achieve

$$\begin{aligned} Res_i(\vartheta,\rho,\tau) =& \varphi_i(\vartheta,\rho,\tau) - \Big[G(\vartheta,\rho,\tau) + E^{-1}[\vartheta^\delta E[\mathcal{L}(\varphi_{i-1}(\vartheta,\rho,\tau)) \\ &+ \mathcal{N}(\varphi_{i-1}(\vartheta,\rho,\tau)) + \upsilon(\varphi_(i-1)(\vartheta,\rho,\tau))]]\Big]. \end{aligned} \tag{2.17}$$

Then

$$Res_m(\vartheta,\rho,\tau) \mid_{\tau=0} = 0,\ \tau \in N^*. \tag{2.18}$$

$Res_m(\vartheta;\rho;\tau)$ is the residual function of Eq. (2.11) and is used to determine the result of $f_m(\vartheta;\rho)(m \in N^*)$.

In this case, ERPSM will provide the approximate i^{th}-order solutions with

$$S_i = \varphi_0 + \varphi_1 + \varphi_3 + \cdots + \varphi_i, \tag{2.19}$$

where

$$\begin{aligned} \varphi_0 &= f_0(\vartheta,\rho), \\ \varphi_1 &= f_1(\vartheta,\rho)\frac{\tau^\delta}{\Gamma(1+2\delta)}, \\ \varphi_2 &= f_2(\vartheta,\rho)\frac{\tau^{2\delta}}{\Gamma(1+2\delta)}, \\ &\vdots \\ \varphi_i &= f_i(\vartheta,\rho)\frac{\tau^{i\delta}}{\Gamma(1+i\delta)}. \end{aligned} \tag{2.20}$$

Remark $R^{\sim}es(\vartheta;\rho;\tau)\mid_{exact}$ generally equals zero for all $\tau\in(0;1]$.$\mid R^{\sim}es_i(\vartheta;\rho;\tau)\mid$ can represent the difference between the precise and approximate solutions. One way to define $\mid R^{\sim}es_i(\vartheta;\rho;\tau)\mid$ is as follows:

$$\mid R^{\sim}es_i(\vartheta;\rho;\tau)\mid=\mid D^{\delta}_{\tau}\varphi_i(\vartheta;\rho;\tau)-(\varphi_i^2(\vartheta;\rho;\tau))_{\vartheta\vartheta}-(\varphi_i^2(\vartheta,\rho,\tau))_{\rho\rho}-\upsilon\varphi_i(\vartheta;\rho;\tau)\mid. \tag{2.21}$$

New itrartive method. See [15,25] for further information on the NIM concept. To solve the following differential equation with an unknown function φ satisfying

$$\varphi=N(\varphi)+f, \tag{2.22}$$

where N is a nonlinear operator and f is a given function. The functions $(\varphi_i)_i$ are found in a series such that $\varphi=\sum_{i=0}^{N}\varphi_i$. The nonlinear operator N can be decomposed using NIM in the following way

$$N\Big(\sum_{i=0}^{\infty}\varphi_i\Big)=N(\varphi_0)+\sum_{i=1}^{\infty}\Bigg[N\Big(\sum_{j=1}^{i}\varphi_j\Big)-N\Big(\sum_{j=0}^{i-1}\varphi_j\Big)\Bigg]. \tag{2.23}$$

By Eq. (2.22) we obtain

$$N\Big(\sum_{i=0}^{\infty}\varphi_i\Big)=f+N(\varphi_0)+\sum_{i=1}^{\infty}\Bigg[N\Big(\sum_{j=0}^{i}\varphi_j\Big)-N\Big(\sum_{j=0}^{i-1}\varphi_j\Big)\Bigg]. \tag{2.24}$$

In light of the recurrence relation that follows,

$$\begin{aligned}
&\varphi_0=f,\\
&\varphi_1=N(\varphi_0),\\
&\varphi_{n+1}=N(\varphi_0+\cdots+\varphi_n)-N(\varphi_0+\cdots+\varphi_(n-1)),\quad n\in\mathbf{N}-0.
\end{aligned}$$

Then

$$(\varphi_n+\cdots+\varphi_{n+1})=N(\varphi_1+\cdots+\varphi_n).$$

Consequently, the following can be used to represent the solution to Eq. (2.22):

$$\varphi=f+\sum_{i=0}^{\infty}\varphi_i.$$

Novel Elzaki iterative method. We consider the following equation to demonstrate the fundamental concept of the NEIM

$$D^m_{\tau}\varphi(\vartheta,\tau)+R\varphi(\vartheta,\tau)=g(\vartheta,\tau),\ m\in\mathbf{N}, \tag{2.25}$$

$$\varphi(\vartheta,0)=h^0(\vartheta),\quad \frac{\partial^k\varphi(\vartheta,0)}{\partial\tau^k}=h^k(\vartheta),\quad k\in(1,\cdots,m-1). \tag{2.26}$$

A general nonlinear operator R, a continuous function g, and the equation $D^m_{\tau}=\frac{\partial^m}{\partial\tau^m}$ are used.

Elzaki transform step. When we apply the Elzaki transform to (2.25), on both sides, we obtain

$$E(\varphi(\vartheta,\tau))-s^m\sum_{k=0}^{m-1}s^{2-m+k}\frac{\partial^k\varphi(\vartheta,0)}{\partial\tau^k}+s^{\tau}E(Ru(\vartheta,\tau)-g(\vartheta,\tau))=0.$$

Applying the initial conditions (2.26) results in

$$\varphi(\vartheta,\tau) = E^{-1}\Big[s^m \sum_{k=0}^{m-1} s^{2-m+k} h^k(\vartheta)\Big] - E^{-1}\Big[s^m E(R\varphi(\vartheta,\tau) - g(\vartheta,\tau))\Big].$$

As a result, we get the usual form shown below

$$\varphi(\vartheta,\tau) = f(\vartheta,\tau) + N[\varphi(\vartheta,\tau)], \tag{2.27}$$

with $f(\vartheta,\tau) = E^{-1}[s^m \sum_{k=0}^{m-1} s^{2-m+k} h^k(\vartheta)]$ and $N[\varphi(\vartheta,\tau)] = -E^{-1}[s^m E(R\varphi(\vartheta,\tau) - g(\vartheta,\tau))]$. The nonlinear portion of the equation is represented by N, and the function f is dependent on the initial conditions.

Remark 4.1. Nothing at all about the duality of the Laplace transform $\mathcal{L}$ and Elzaki transform E.

$$E(f)(s) = s\mathcal{L}(f)(\frac{1}{s}) \text{ and } \mathcal{L}(f)(s) = sE(f)\frac{1}{s}.$$

The following inversion formula is so easily obtained

$$f(\tau) = \frac{1}{2\pi}\int_{\delta-\iota\infty}^{\delta-\iota\infty} sE(f)(\frac{1}{s})\exp(s\tau)ds. \tag{2.28}$$

Iterative method step. We get at the resulting algorithm using the iterative approach described in Section 'New iterative method' on the problem (2.27).

$$\begin{aligned}
&\varphi_0 = f,\\
&\varphi_1 = N(\varphi_0),\\
&\varphi_{n+1} = N(\varphi_0 + \cdots + \varphi_n) - N(\varphi_o + \cdots + \varphi_{n-1}), \ \ n \in \mathbf{N} - 0,
\end{aligned}$$

therefore $\varphi = \sum_{m=1}^{\infty} \varphi_i$ is obtained.

2.1. Problem 1

2.1.1. Implementation of ERPSM

In this section, we apply ERPSM to understand the anomalous behavior of the fractional-order Broer-Kaup (BK) system, which is given by

$$\begin{aligned}
&D_t^\delta \varphi(\vartheta,\tau) + \varphi(\vartheta,\tau)\varphi(\vartheta,\tau)_\vartheta + \phi(\vartheta,\tau)_\vartheta = 0,\\
&D_t^\delta \phi(\vartheta,\tau) + \varphi(\vartheta,\tau)_\vartheta + \varphi(\vartheta,\tau)\phi(\vartheta,\tau)_\vartheta + \phi(\vartheta,\tau)\varphi(\vartheta,\tau)_\vartheta\\
&+ \varphi(\vartheta,\tau)_{\vartheta\vartheta\vartheta} = 0, \quad \text{where } \tau > 0, \ \ \varphi,\phi \in \Re, \ \ 0 < \delta \le 1.
\end{aligned} \tag{2.29}$$

The following ICs are applicable:

$$\begin{aligned}
\varphi(\vartheta,\tau) &= 2\tanh(\vartheta) + 1,\\
\phi(\vartheta,\tau) &= 1 - 2\tanh^2(\vartheta).
\end{aligned} \tag{2.30}$$

The exact solution is given as:

$$\begin{aligned}
\varphi(\vartheta,\tau) &= 1 - 2\tanh(\tau - \vartheta),\\
\phi(\vartheta,\tau) &= 1 - 2\tanh^2(\tau - \vartheta).
\end{aligned} \tag{2.31}$$

Using Eq. (2.30) and applying ET to Eq. (2.29) we obtain:

$$\begin{aligned}&\varphi(\vartheta,s)-(2\tanh(\vartheta)+1)s^2+s^{\delta}E_\tau[E_\tau^{-1}\varphi(\vartheta,s)(E_\tau^{-1}\varphi(\vartheta,s)_\vartheta)]=0,\\&\phi(\vartheta,s)-(1-2\tanh^2(\vartheta))s^2+s^{\delta}E_\tau[E_\tau^{-1}\varphi(\vartheta,s)(E_\tau^{-1}\phi(\vartheta,s)_\vartheta)]\\&+s^{\delta}E_\tau[E_\tau^{-1}\phi(\vartheta,s)(E_\tau^{-1}\varphi(\vartheta,s)_\vartheta)]+s^{\delta}[\varphi(\vartheta,s)_\vartheta]+s^{\delta}[\varphi(\vartheta,s)_{\vartheta\vartheta\vartheta}=0.\end{aligned}\tag{2.32}$$

Thus, the term series that are k^{th}-truncated are:

$$\begin{aligned}\varphi(\vartheta,s)&=s^2(2\tanh(\vartheta)+1)+\sum_{r=1}^{k}\frac{f_r(\vartheta,s)}{(s^{r\delta+1})},\quad r=1,2,3,4\cdots,\\\phi(\vartheta,s)&=s^2(1-2\tanh^2(\vartheta))+\sum_{r=1}^{k}\frac{f_r(\vartheta,s)}{(s^{r\delta+1})},\quad r=1,2,3,4\cdots.\end{aligned}\tag{2.33}$$

The Elzaki residual functions (ERFs) are provided as follows:

$$\begin{aligned}E_\tau Res\varphi(\vartheta,s)&=\varphi(\vartheta,s)-(2\tanh(\vartheta)+1)s^2+s^{\delta}E_\tau[E_\tau^{-1}\varphi(\vartheta,s)(E_\tau^{-1}\varphi(\vartheta,s)_\vartheta)]=0,\\E_\tau Res\phi(\vartheta,s)&=\phi(\vartheta,s)-(1-2\tanh^2(\vartheta))s^2+s^{\delta}E_\tau[E_\tau^{-1}\varphi(\vartheta,s)(E_\tau^{-1}\phi(\vartheta,s)_\vartheta)]\\&\quad+s^{\delta}E_\tau[E_\tau^{-1}\phi(\vartheta,s)(E_\tau^{-1}\varphi(\vartheta,s)_\vartheta)]\\&\quad+s^{\delta}[\varphi(\vartheta,s)_\vartheta]+s^{\delta}[\varphi(\vartheta,s)_{\vartheta\vartheta\vartheta}\\&=0.\end{aligned}\tag{2.34}$$

Along with the k^{th}-ERFs as:

$$\begin{aligned}E_\tau Res(\varphi_k(\vartheta,s))&=\varphi_k(\vartheta,s)-(2\tanh(\vartheta)+1)s^2\\&\quad+s^{\delta}E_\tau[E_\tau^{-1}\varphi_k(\vartheta,s)(E_\tau^{-1}\varphi_k(\vartheta,s)_\vartheta)]\\&=0,\\E_\tau Res\phi_k(\vartheta,s)&=\phi_k(\vartheta,s)-(1-2\tanh^2(\vartheta))s^2\\&\quad+s^{\delta}E_\tau[E_\tau^{-1}\varphi_k(\vartheta,s)(E_\tau^{-1}\phi_k(\vartheta,s)_\vartheta)]\\&\quad+s^{\delta}E_\tau[E_\tau^{-1}\phi_k(\vartheta,s)(E_\tau^{-1}\varphi_k(\vartheta,s)_\vartheta)]\\&\quad+s^{\delta}[\varphi_k(\vartheta,s)_\vartheta]+s^{\delta}[\varphi_k(\vartheta,s)_{\vartheta\vartheta\vartheta}\\&=0.\end{aligned}\tag{2.35}$$

To find $f_r(\vartheta,s)$ now, $r=1,2,3,\cdots$. We multiply the resulting equation by $s^{r\delta+1}$, substitute the $r^{\tau h}$-truncated series Eq. (2.34) into the $r^{\tau h}$-Elzaki residual function Eq. (2.35) and solve the relation

$\lim_{s\to\infty}(s^{r\delta+1}\mathcal{L}_\tau Res_{\vartheta,r}(\tau,s))=0$ and $\lim_{s\to\infty}(s^{r\delta+1}\mathcal{L}_\tau Res_{\rho,r}(\tau,s))=0$ recursively. $1,2,3,\cdots$. Here are the first few terms:

$$\begin{aligned}f_1(\vartheta,s)&=-2\operatorname{sech}^2(\vartheta),\\g_1(\vartheta,s)&=4\tanh(\vartheta)\operatorname{sech}^2(\vartheta),\end{aligned}\tag{2.36}$$

$$\begin{aligned}f_2(\vartheta,s)&=-4\tanh(\vartheta)\operatorname{sech}^2(\vartheta),\\g_2(\vartheta,s)&=4(\cosh(2\vartheta)-2)\operatorname{sech}^4(\vartheta),\end{aligned}\tag{2.37}$$

and so on.

Using $f_r(\vartheta, s)$ and $g_r(\vartheta, s)$ $r = 1, 2, 3, \cdots$, as the values in Eq. (2.33) we obtain:

$$\begin{aligned} \varphi(\vartheta,\tau) &= \frac{1+2\tanh(\vartheta)}{s} - \frac{2\operatorname{sech}^2(\vartheta)}{s^{\delta+1}} - \frac{4\tanh(\vartheta)\operatorname{sech}^2(\vartheta)}{s^{2\delta+1}}, \\ \phi(\vartheta,\tau) &= \frac{1-2\tanh^2(\vartheta)}{s} + \frac{4(\cosh(2\vartheta)-2)\operatorname{sech}^4(\vartheta)}{s^{2\delta+1}} + \frac{4\tanh(\vartheta)\operatorname{sech}^2(x)}{s^{\delta+1}}. \end{aligned} \tag{2.38}$$

With the inverse Elzaki transform, we obtain

$$\begin{aligned} \varphi(\vartheta,\tau) &= 1+2\tanh(\vartheta) - \frac{4\tau^{2\delta}\tanh(\vartheta)\operatorname{sech}^2(\vartheta)}{\Gamma(2\delta+1)} - \frac{2\tau^{\delta}\operatorname{sech}^2(\vartheta)}{\Gamma(\delta+1)} + \cdots, \\ \phi(\vartheta,\tau) &= 1-2\tanh^2(\vartheta) - \frac{8\tau^{2\delta}\operatorname{sech}^4(\vartheta)}{\Gamma(2\delta+1)} + \frac{4\tau^{2\delta}\cosh(2\vartheta)\operatorname{sech}^4(\vartheta)}{\Gamma(2\delta+1)} \\ &\quad + \frac{4\tau^{\delta}\tanh(\vartheta)\operatorname{sech}^2(\vartheta)}{\Gamma(\delta+1)} + \cdots. \end{aligned} \tag{2.39}$$

Table 1. Using ERPSM solution to find the various values for $\tau = 0.3$ of $\varphi(\vartheta, \tau)$.

ϑ	$ERPSM_{\delta=0.6}$	$ERPSM_{\delta=0.8}$	$ERPSM_{\delta=1}$	$Exact_{\delta=1}$	$AbsoluteError_{\delta=1}$
0.	0.85877	0.946061	0.98	0.980001	6.66640×10^{-7}
0.1	1.05808	1.14576	1.17951	1.17952	6.41645×10^{-7}
0.2	1.25628	1.34258	1.37549	1.37549	5.68179×10^{-7}
0.3	1.44953	1.53279	1.56427	1.56427	4.57860×10^{-7}
0.4	1.63436	1.71317	1.74272	1.74272	3.26777×10^{-7}
0.5	1.80791	1.88117	1.90843	1.90843	1.91701×10^{-7}
0.6	1.96808	2.03504	2.05979	2.05979	6.68165×10^{-7}
0.7	2.11355	2.17382	2.19596	2.19596	3.82057×10^{-7}
0.8	2.24375	2.29726	2.31682	2.31682	1.18632×10^{-7}
0.9	2.35879	2.40572	2.42279	2.42279	1.73963×10^{-7}
1.	2.45925	2.49997	2.51472	2.51472	2.06645×10^{-7}

Table 2. Using ERPSM solution to find the various values for $\tau = 0.2$ of $\phi(\vartheta, \tau)$.

ϑ	$ERPSM_{\delta=0.6}$	$ERPSM_{\delta=0.8}$	$ERPSM_{\delta=1}$	$Exact_{\delta=1}$	$AbsoluteError_{\delta=1}$
0.1	0.994122	0.989082	0.983888	0.983887	5.06170×10^{-7}
0.2	0.963398	0.941051	0.929504	0.929503	9.43252×10^{-7}
0.3	0.895716	0.857829	0.840801	0.8408	1.23564×10^{-6}
0.4	0.796095	0.745492	0.724185	0.724183	1.35748×10^{-6}
0.5	0.671466	0.611603	0.587376	0.587375	1.32006×10^{-6}
0.6	0.529713	0.464212	0.438422	0.438421	1.16145×10^{-6}
0.7	0.378714	0.31097	0.284836	0.284835	9.31235×10^{-7}
0.8	0.225578	0.158477	0.132996	0.132995	6.76697×10^{-7}
0.9	0.0761456	0.0119236	-0.0121616	-0.0121621	4.34223×10^{-7}
1.	-0.0652141	-0.124998	-0.147195	-0.147195	2.26350×10^{-7}

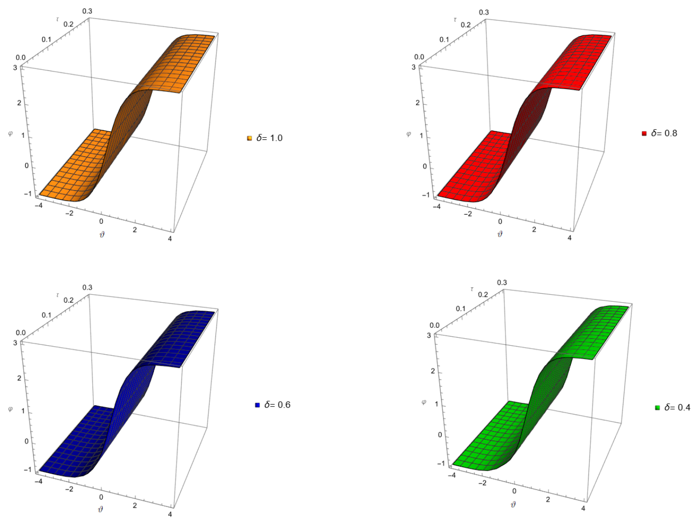

Figure 1. In Figure 1, ERPSM solution for (a), (b), (c) and (d) shows that fractional order at $\delta = 1$, $\delta = 0.8$, $\delta = 0.6$, and $\delta = 0.4$ for $\tau = 0.3$ of $\varphi(\vartheta, \tau)$.

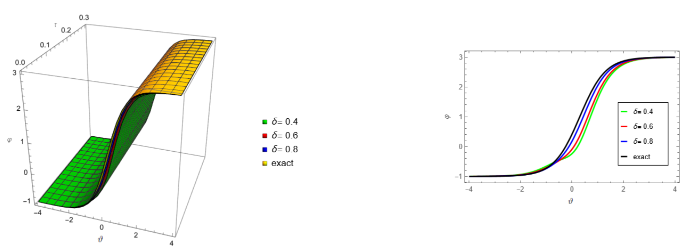

Figure 2. In Figure 2, Comparison between ERPSM solution and exact for 3D plot of $\varphi(\vartheta, \tau)$ for $\tau = 0.3$ for various fractional order values of $\delta = 1$, $\delta = 0.8$, $\delta = 0.6$, and $\delta = 0.4$.

2.1.2. Implementation of NITM

We derive the corresponding form given below by applying the RL integral on Eq. (2.29):

$$\begin{aligned} \varphi(\vartheta,\tau) &= 2\tanh(\vartheta) + 1 - \mathfrak{R}_\tau^\delta \left[-\varphi(\vartheta,\tau)\varphi(\vartheta,\tau)_\vartheta - \phi(\vartheta,\tau)_\vartheta\right], \\ \phi(\vartheta,\tau) &= 1 - 2\tanh^2(\vartheta) - \mathfrak{R}_\tau^\delta \left[-\varphi(\vartheta,\tau)_\vartheta \right. \\ &\qquad \left. -\varphi(\vartheta,\tau)\phi(\vartheta,\tau)_\vartheta - \phi(\vartheta,\tau)\varphi(\vartheta,\tau)_\vartheta - \varphi(\vartheta,\tau)_{\vartheta\vartheta\vartheta}\right]. \end{aligned} \tag{2.40}$$

We obtain the following several terms based on the NITM procedure:

$$\begin{aligned} f_0(\vartheta,\tau) &= 2\tanh(\vartheta) + 1, \\ f_1(\vartheta,\tau) &= -\frac{2\tau^\delta \operatorname{sech}^2(x)}{\delta\Gamma(\delta)}, \\ f_2(\vartheta,\tau) &= -\frac{4\tau^{2\delta}\tanh(\vartheta)\operatorname{sech}^2(\vartheta)\left(\Gamma(\delta+1) - 2\tau^\delta \operatorname{sech}^2(\vartheta)\right)}{\Gamma(\delta+1)^3}, \end{aligned} \tag{2.41}$$

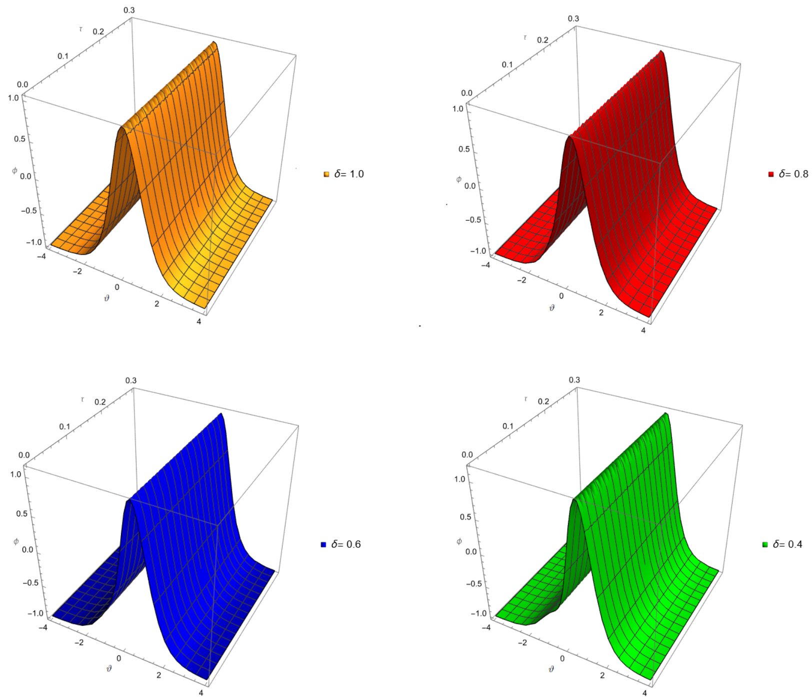

Figure 3. In Figure 3, ERPSM solution for (a), (b), (c) and (d) shows that fractional order at $\delta = 1$, $\delta = 0.8$, $\delta = 0.6$, and $\delta = 0.4$ for $\tau = 0.3$ of $\phi(\vartheta, \tau)$.

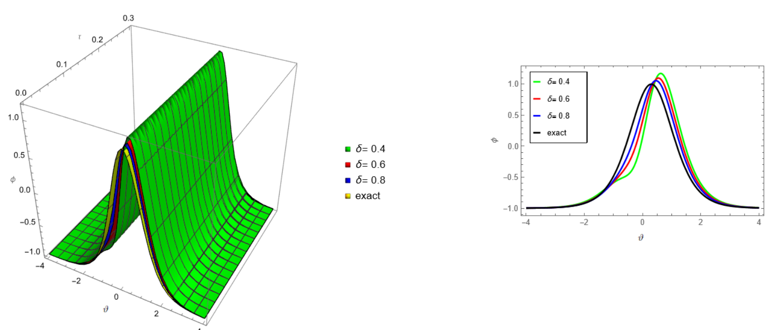

Figure 4. In Figure 4, comparison between ERPSM solution and exact for 3D plot of $\phi(\vartheta, \tau)$ for $\tau = 0.3$ for various fractional order values of $\delta = 1$, $\delta = 0.8$, $\delta = 0.6$, and $\delta = 0.4$.

$$
\begin{aligned}
g_0(\vartheta, \tau) &= 1 - 2\tanh^2(\vartheta), \\
g_1(\vartheta, \tau) &= \frac{4\tau^p \tanh(\vartheta)\operatorname{sech}^2(\vartheta)}{\delta\Gamma(\delta)}, \\
g_2(\vartheta, \tau) &= \frac{4\tau^{2\delta}\operatorname{sech}^4(\vartheta)\left(2\tau^\delta\left(5\operatorname{sech}^2(\vartheta) - 4\right) + \delta\Gamma(\delta)(\cosh(2\vartheta) - 2)\right)}{\Gamma(\delta+1)^3}.
\end{aligned}
\tag{2.42}
$$

The final NITM algorithm solution is as follows:

$$\varphi(\vartheta, \tau) = \varphi_0(\vartheta, \tau) + \varphi_1(\vartheta, \tau) + \varphi_2(\vartheta, \tau) + \cdots, \tag{2.43}$$

$$\phi(\vartheta, \tau) = \phi_0(\vartheta, \tau) + \phi_1(\vartheta, \tau) + \phi_2(\vartheta, \tau) + \cdots, \tag{2.44}$$

$$\varphi(\vartheta,\tau) = 1 + 2\tanh(\vartheta) - \frac{2\tau^{\delta}\operatorname{sech}^2(\vartheta)}{\delta\Gamma(\delta)} - \frac{4\tau^{2\delta}\tanh(\vartheta)\operatorname{sech}^2(\vartheta)\left(\Gamma(\delta+1) - 2\tau^{\delta}\operatorname{sech}^2(\vartheta)\right)}{\Gamma(\delta+1)^3} + \cdots, \tag{2.45}$$

$$\phi(\vartheta,\tau) = 1 - 2\tanh^2(\vartheta) + \frac{4\tau^{\delta}\tanh(\vartheta)\operatorname{sech}^2(\vartheta)}{\delta\Gamma(\delta)} + \frac{4\tau^{2\delta}\operatorname{sech}^4(\vartheta)\left(2\tau^{\delta}\left(5\operatorname{sech}^2(\vartheta) - 4\right) + \delta\Gamma(\delta)(\cosh(2\vartheta) - 2)\right)}{\Gamma(\delta+1)^3} + \cdots. \tag{2.46}$$

Table 3. Using NITM solution to find the various values for $\tau = 0.3$ of $\varphi(\vartheta,\tau)$.

ϑ	$NITM_{\delta=0.6}$	$NITM_{\delta=0.8}$	$NITM_{\delta=1}$	$Exact_{\delta=1.0}$	$AbsoluteError_{\delta=1.0}$.
0.	0.85877	0.946061	0.98	0.980001	6.66640×10^{-7}
0.1	1.05782	1.14566	1.1795	1.17952	1.95956×10^{-5}
0.2	1.25575	1.34239	1.37546	1.37549	3.7047×10^{-5}
0.3	1.44875	1.53253	1.56422	1.56427	5.18243×10^{-5}
0.4	1.63335	1.71284	1.74266	1.74272	6.31213×10^{-5}
0.5	1.80672	1.8808	1.90836	1.90843	7.05913×10^{-5}
0.6	1.96675	2.03465	2.05972	2.05979	7.43219×10^{-5}
0.7	2.11213	2.17342	2.19589	2.19596	7.47371×10^{-5}
0.8	2.2423	2.29687	2.31675	2.31682	7.24677×10^{-5}
0.9	2.35735	2.40534	2.42272	2.42279	6.8223×10^{-5}
1.	2.45787	2.49963	2.51466	2.51472	6.26887×10^{-5}

Table 4. Using NITM solution to find the various values for $\tau = 0.3$ of $\phi(\vartheta,\tau)$.

ϑ	$NITM_{\delta=0.6}$	$NITM_{\delta=0.8}$	$NITM_{\delta=1}$	$Exact_{\delta=1.0}$	$AbsoluteError_{\delta=1.0}$.
0.	0.982871	0.997248	0.999608	0.9998	1.92013×10^{-4}
0.1	0.99147	0.988129	0.983703	0.983887	1.84154×10^{-4}
0.2	0.960831	0.940196	0.92934	0.929503	1.62852×10^{-4}
0.3	0.893327	0.857124	0.840669	0.8408	1.31338×10^{-4}
0.4	0.794004	0.744969	0.724089	0.724183	9.40283×10^{-5}
0.5	0.669796	0.611273	0.587319	0.587375	5.55361×10^{-5}
0.6	0.528556	0.464067	0.438401	0.438421	1.98041×10^{-5}
0.7	0.37811	0.310987	0.284845	0.284835	1.04272×10^{-5}
0.8	0.225508	0.158624	0.133029	0.132995	3.37609×10^{-5}
0.9	0.0765425	0.0121657	-0.0121121	-0.0121621	4.99789×10^{-5}
1.	-0.0644509	-0.124695	-0.147136	-0.147195	5.97079×10^{-5}

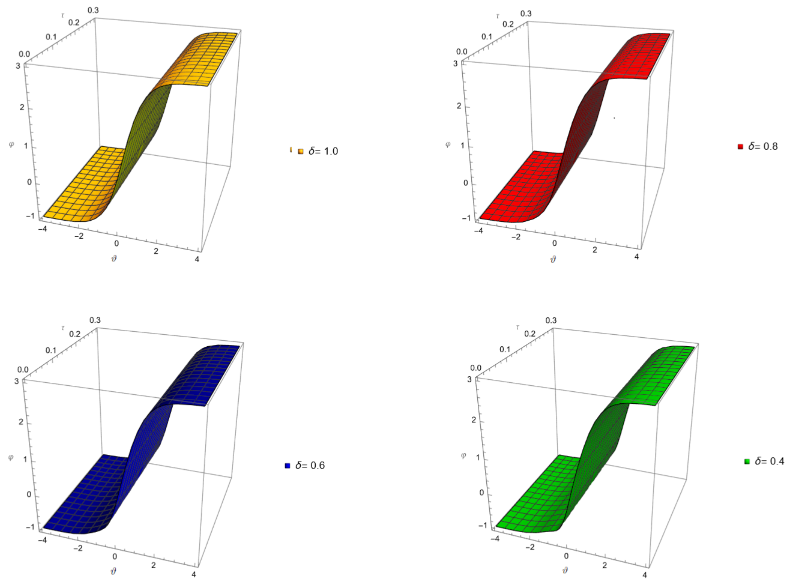

Figure 5. In Figure 5, NITM solution for (a), (b), (c) and (d) shows that fractional order at $\delta = 1$, $\delta = 0.8$, $\delta = 0.6$, and $\delta = 0.4$ for $\tau = 0.3$ of $\varphi(\vartheta, \tau)$.

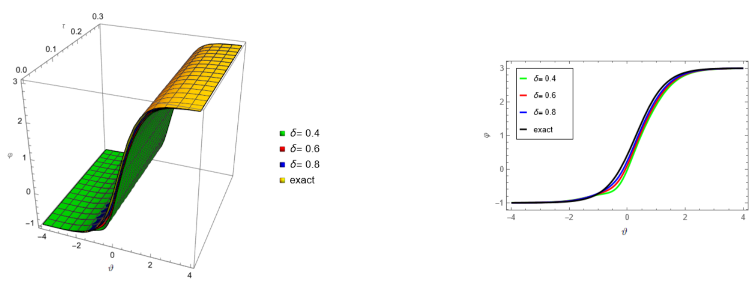

Figure 6. In Figure 6, comparison between NITM solution and exact for 3D plot of $\varphi(\vartheta, \tau)$ for $\tau = 0.3$ for various fractional order values of $\delta = 1$, $\delta = 0.8$, $\delta = 0.6$, and $\delta = 0.4$.

3. Graphical and tables discussion

The graphical representations and tables presented in this study provide a comprehensive analysis of the solutions obtained for the fractional-order Whitham-Broer-Kaup (WBK) system using the Elzaki Residual Power Series Method (ERPSM) and the New Iteration Transform Method (NITM). These visualizations and data tables offer valuable insights into the behavior of the system under various fractional orders and facilitate a comparative evaluation of the two methods.

Figure 1: This figure illustrates the ERPSM solutions for the variable $\varphi(\vartheta, \tau)$ at $\tau = 0.3$ across different fractional orders: (a) $\delta = 1$, (b) $\delta = 0.8$, (c) $\delta = 0.6$, and (d) $\delta = 0.4$. The plots reveal that as the fractional order δ decreases, the amplitude and wave profiles of $\varphi(\vartheta, \tau)$ undergo significant changes, indicating the influence of fractional differentiation on the system's dynamics. Figure 2: This

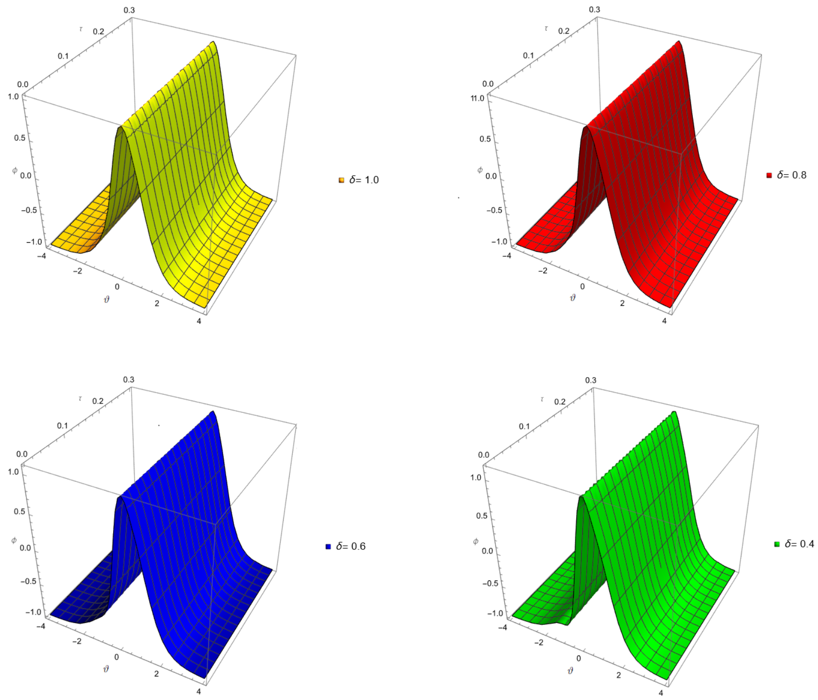

Figure 7. In Figure 7, NITM solution for (a), (b), (c) and (d) shows that fractional order at $\delta = 1$, $\delta = 0.8$, $\delta = 0.6$, and $\delta = 0.4$ for $\tau = 0.3$ of $\phi(\vartheta, \tau)$.

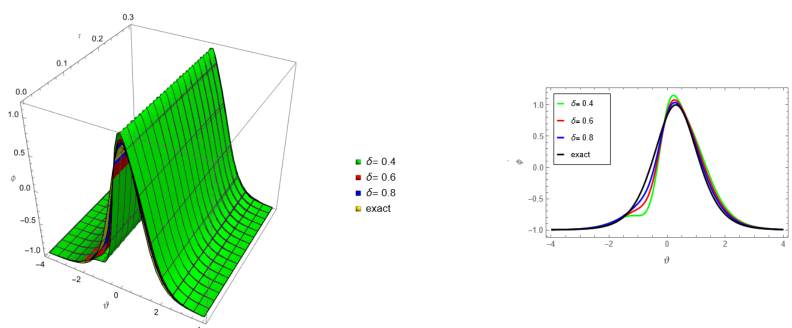

Figure 8. In Figure 8, comparison between NITM solution and exact for 3D plot of $\phi(\vartheta, \tau)$ for $\tau = 0.3$ for various fractional order values of $\delta = 1$, $\delta = 0.8$, $\delta = 0.6$, and $\delta = 0.4$.

figure presents a comparison between the ERPSM solutions and the exact solutions for $\varphi(\vartheta, \tau)$ at $\tau = 0.3$ for various fractional orders $\delta = 1$, $\delta = 0.8$, $\delta = 0.6$, and $\delta = 0.4$. The close alignment between the ERPSM and exact solutions across all cases demonstrates the accuracy and reliability of the ERPSM in approximating the behavior of the fractional WBK system. Figure 3: Similar to Figure 1, this figure depicts the ERPSM solutions for $\varphi(\vartheta, \tau)$ at $\tau = 0.3$ for fractional orders: (a) $\delta = 1$, (b) $\delta = 0.8$, (c) $\delta = 0.6$, and (d) $\delta = 0.4$. The observed variations in wave structures with changing δ values further emphasize the role of fractional order in shaping the system's responses. Figure 4: This figure compares the ERPSM solutions with exact solutions for $\varphi(\vartheta, \tau)$ at $\tau = 0.3$ across the specified fractional orders. The high degree of correlation between the two sets of solutions reaffirms the effectiveness of ERPSM in capturing the essential dynamics of the fractional WBK system. Figure 5: This figure showcases the NITM solutions for $\varphi(\vartheta, \tau)$ at $\tau = 0.3$ for fractional orders: (a) $\delta = 1$, (b) $\delta = 0.8$, (c) $\delta = 0.6$, and (d) $\delta = 0.4$. The results indicate that NITM effectively models the system's behavior, with noticeable changes in wave patterns corresponding to different δ values. Figure 6: This figure provides a comparative analysis between the NITM solutions and exact solutions for $\varphi(\vartheta, \tau)$ at $\tau = 0.3$ for various fractional orders. The agreement between the NITM and exact solutions underscores the precision of NITM in solving the fractional WBK equations. Figure 7: Depicting the NITM solutions for $\varphi(\vartheta, \tau)$ at $\tau = 0.3$ for fractional orders: (a) $\delta = 1$, (b) $\delta = 0.8$, (c) $\delta = 0.6$, and (d) $\delta = 0.4$, this figure highlights the method's capability to adapt to varying fractional orders and accurately represent the system's dynamics. Figure 8: This figure compares the NITM solutions with exact solutions for $\varphi(\vartheta, \tau)$ at $\tau = 0.3$ across different fractional orders. The close match between the solutions validates the robustness of NITM in addressing the complexities of the fractional WBK system.

Table 1: This table presents the computed values of $\varphi(\vartheta, \tau)$ using ERPSM at $\tau = 0.3$ for various values. The data demonstrate the method's consistency and accuracy across different fractional orders. Table 2: Displaying the ERPSM-derived values for $\varphi(\vartheta, \tau)$ at $\tau = 0.2$, this table further confirms the reliability of ERPSM in producing precise solutions for the fractional WBK system. Table 3: This table shows the NITM solutions for $\varphi(\vartheta, \tau)$ at $\tau = 0.3$, highlighting the method's effectiveness in handling fractional-order computations. Table 4: Providing the NITM-derived values for $\varphi(\vartheta, \tau)$ at $\tau = 0.2$, this table corroborates the accuracy of NITM in solving the fractional WBK equations.

In summary, the figures and tables collectively demonstrate that both ERPSM and NITM are potent analytical tools for solving the fractional-order WBK system. The visual and numerical data highlight how varying the fractional order δ influences the system's behavior, offering deeper insights into the dynamics of nonlinear wave models. The comparative analyses with exact solutions affirm the accuracy and applicability of these methods in the realm of fractional calculus and its applications in mathematical physics and engineering.

4. Conclusion

In this paper, the Elzaki residual power series method (ERPSM) and New iteration transform method (NITM) to the investigate fractional-order Whitham-Broer-Kaup system. Some of the most important nonlinear fractional differential equations in wave movements and fluid mechanics were transformed and simplified efficiently to extract accurate analytical solutions. It was clear from the analysis that the proposed methods are robust, efficient and to some extent, very simple for solutions to complex fractional-order systems. For these methods, both convergence analysis and numerical simulations were conducted. The results showcased intricate wave behaviors and highly precise nonlinear dynamics, validating the claims made regarding the effectiveness of ERPSM and NITM. Both methods characteristically solved problems regarding fractional-order systems, establishing a standard for mathematicians and engineers of mathematical physics and applied sciences making them adaptable and reliable. The results optimize the study of fractional-order models, suggesting that both methods could be used for further research. Expansion of this research could include multi-dimensional system with coupled equations and other nonlinear models to explore more phenomena in fractional calculus and nonlinear dynamics.

Acknowledgments

This work was supported by the Deanship of Scientific Research, Vice Presidency for Graduate Studies and Scientific Research, King Faisal University, Saudi Arabia (Grant No. KFU252477). Princess Nourah bint Abdulrahman University Researchers Supporting Project number (PNURSP2025R183), Princess Nourah bint Abdulrahman University, Riyadh, Saudi Arabia.

Funding

This work was supported by the Deanship of Scientific Research, Vice Presidency for Graduate Studies and Scientific Research, King Faisal University, Saudi Arabia (Grant No. KFU252477). Princess Nourah bint Abdulrahman University Researchers Supporting Project number (PNURSP2025R183), Princess Nourah bint Abdulrahman University, Riyadh, Saudi Arabia.

References

[1] G. Adomian, *Solving Frontier Problems of Physics: The Decomposition Method (Vol. 60)*, Springer Science and Business Media, 2013.

[2] A. El-Ajou, *Adapting the Laplace transform to create solitary solutions for the nonlinear time-fractional dispersive PDEs via a new approach*, The European Physical Journal Plus, 2021, 136(2), 229.

[3] A. El-Ajou, O. A. Arqub and S. Momani, *Approximate analytical solution of the nonlinear fractional KdV-Burgers equation: A new iterative algorithm*, Journal of Computational Physics, 2015, 293, 81–95.

[4] A. El-Ajou, O. A. Arqub and S. Momani, *Approximate analytical solution of the nonlinear fractional KdV-Burgers equation: A new iterative algorithm*, Journal of Computational Physics, 2015, 293, 81–95.

[5] A. El-Ajou and Z. Al-Zhour, *A vector series solution for a class of hyperbolic system of Caputo time-fractional partial differential equations with variable coefficients*, Frontiers in Physics, 2021, 9, 525250.

[6] A. Akgul, *A novel method for a fractional derivative with non-local and non-singular kernel*, Chaos, Solitons and Fractals, 2018, 114, 478–482.

[7] E. K. Akgul, *Solutions of the linear and nonlinear differential equations within the generalized fractional derivatives*, Chaos: An Interdisciplinary Journal of Nonlinear Science, 2019, 29(2).

[8] A. A. Alderremy, N. Iqbal, S. Aly and K. Nonlaopon, *Fractional series solution construction for nonlinear fractional reaction-diffusion Brusselator model utilizing Laplace residual power series*, Symmetry, 2022, 14(9), 1944.

[9] A. Ali, K. Shah and R. A. Khan, *Numerical treatment for traveling wave solutions of fractional Whitham-Broer-Kaup equations*, Alexandria Engineering Journal, 2018, 57(3), 1991–1998.

[10] M. Alqhtani, K. M. Saad, R. Shah and W. M. Hamanah, *Discovering novel soliton solutions for (3+1)-modified fractional Zakharov-Kuznetsov equation in electrical engineering through an analytical approach*, Optical and Quantum Electronics, 2023, 55(13), 1149.

[11] M. Alqhtani, K. M. Saad, R. Shah, W. Weera and W. M. Hamanah, *Analysis of the fractional-order local Poisson equation in fractal porous media*, Symmetry, 2022, 14(7), 1323.

[12] A. Atangana, *Fractal-fractional differentiation and integration: Connecting fractal calculus and fractional calculus to predict complex system*, Chaos, Solitons and Fractals, 2017, 102, 396–406.

[13] D. Baleanu, K. Diethelm, E. Scalas and J. J. Trujillo, *Fractional Calculus: Models and Numerical Methods (Vol. 3)*, World Scientific, 2012.

[14] W. Bao, H. Liu, F. Wang, J. Du, Y. Wang, H. Li and X. Ye, *Keyhole critical failure criteria and variation rule under different thicknesses and multiple materials in K-TIG welding,* Journal of Manufacturing Processes, 2024, 126, 48–59.

[15] S. Bhalekar and V. Daftardar-Gejji, *New iterative method: Application to partial differential equations*, Applied Mathematics and Computation, 2008, 203(2), 778–783.

[16] M. Caputo, *Linear models of dissipation whose Q is almost frequency independent-II*, Geophysical Journal International, 1967, 13(5), 529–539.

[17] M. Caputo and M. Fabrizio, *A new definition of fractional derivative without singular kernel*, Progress in Fractional Differentiation and Applications, 2015, 1(2), 73–85.

[18] X. Chen and R. Jing, *Video super resolution based on deformable 3D convolutional group fusion*, Scientific Reports, 2025, 15(1), 9050. DOI: 10.1038/s41598-025-93758-z.

[19] J. Du, H. Liu, F. Wang, W. Bao and H. Li, *Solidification microstructure reconstruction and its effects on phase transformation, grain boundary transformation mechanism, and mechanical properties of TC4 alloy welded joint*, Metallurgical and Materials Transactions A, 2024, 55(4), 1193–1206.

[20] E. M. Elsayed, R. Shah and K. Nonlaopon, *The analysis of the fractional-order Navier-Stokes equations by a novel approach*, Journal of Function Spaces, 2022, 2022(1), 8979447.

[21] T. M. Elzaki, *The new integral transform Elzaki transform*, Global Journal of Pure and Applied Mathematics, 2011, 7(1), 57–64.

[22] T. Eriqat, A. El-Ajou, N. O. Moa'ath, Z. Al-Zhour and S. Momani, *A new attractive analytic approach for solutions of linear and nonlinear neutral fractional pantograph equations*, Chaos, Solitons and Fractals, 2020, 138, 109957.

[23] T. Eriqat, M. A. N. Oqielat, Z. Al-Zhour, A. El-Ajou and A. S. Bataineh, *Revisited Fisher's equation and logistic system model: A new fractional approach*

and some modifications, International Journal of Dynamics and Control, 2023, 11(2), 555–563.

[24] V. Daftardar-Gejji and S. Bhalekar, *Solving fractional diffusion-wave equations using a new iterative method*, Fractional Calculus and Applied Analysis, 2008, 11(2), 193–202.

[25] V. Daftardar-Gejji and H. Jafari, *An iterative method for solving nonlinear functional equations*, Journal of Mathematical Analysis and Applications, 2006, 316(2), 753–763.

[26] V. Daftardar-Gejji and H. Jafari, *An iterative method for solving nonlinear functional equations*, Journal of Mathematical Analysis and Applications, 2006, 316(2), 753–763.

[27] S. Guo, Y. Li and D. Wang, *2-term extended RotaBaxter pre-lie-algebra and non-abelian extensions of extended RotaBaxter pre-lie algebras*, Results in Mathematics, 2025, 80(3), 96. DOI: 10.1007/s00025-025-02411-8.

[28] J. H. He, *Homotopy perturbation technique*, Computer methods in Applied Mechanics and Engineering, 1999, 178(3–4), 257–262.

[29] J. H. He, *Approximate analytical solution for seepage flow with fractional derivatives in porous media*, Computer Methods in Applied Mechanics and Engineering, 1998, 167(1–2), 57–68.

[30] Z. Huang, X. Zheng, C. Li, E. L. Tan, Z. Chen, L. Shi and B. Chen, *Piecewise calculation scheme for the unconditionally stable Chebyshev finite-difference time-domain method*, IEEE Transactions on Microwave Theory and Techniques, 2025, 1–9. DOI: 10.1109/TMTT.2025.3532330.

[31] E. Keshavarz, Y. Ordokhani and M. Razzaghi, *Bernoulli wavelet operational matrix of fractional order integration and its applications in solving the fractional order differential equations*, Applied Mathematical Modelling, 2014, 38(24), 6038–6051.

[32] A. A. Kilbas, H. M. Srivastava and J. J. Trujillo, *Theory and applications of fractional differential equations*, Elsevier, 2006, 204.

[33] J. Li, X. Zhu, C. Feng, M. Wen and Y. Zhang, *A simple and efficient three-dimensional spring element model for pore seepage problems*, Engineering Analysis with Boundary Elements, 2025, 176, 106225.

[34] K. Liu, S. Jiao, G. Nie, H. Ma, B. Gao, C. Sun and G. Wu, *On image transformation for partial discharge source identification in vehicle cable terminals of high-speed trains*, High Voltage, 2024, 9(5), 1090–1100. DOI: 10.1049/hve2.12487.

[35] C. Ma, R. Mu, M. Li, J. He, C. Hua, L. Wang, J. Liu, G. Totis, J. Yang, K. Liu and Y. Zhou, *A multi-scale spatial temporal interaction fusion network for digital twin-based thermal error compensation in precision machine tools*, Expert Systems with Applications, 2025, 127812.

[36] A. M. Malik and O. H. Mohammed, *Two efficient methods for solving fractional Lane-Emden equations with conformable fractional derivative*, Journal of the Egyptian Mathematical Society, 2020, 28, 1–11.

[37] N. O. Moa'ath, A. El-Ajou, Z. Al-Zhour, T. Eriqat and M. Al-Smadi, *A new approach to solving fuzzy quadratic Riccati differential equations*, International Journal of Fuzzy Logic and Intelligent Systems, 2022, 22(1), 23–47.

[38] M. Naeem, O. F. Azhar, A. M. Zidan, K. Nonlaopon and R. Shah, *Numerical analysis of fractional-order parabolic equations via Elzaki transform*, Journal of Function Spaces, 2021, 2021(1), 3484482.

[39] M. Naeem, H. Rezazadeh, A. A. Khammash and S. Zaland, *Analysis of the fuzzy fractional-order solitary wave solutions for the KdV equation in the sense of Caputo-Fabrizio derivative*, Journal of Mathematics, 2022, 2022(1), 3688916.

[40] K. Nonlaopon, M. Naeem, A. M. Zidan, R. Shah, A. Alsanad and A. Gumaei, *Numerical investigation of the time-fractional Whitham-Broer-Kaup equation involving without singular kernel operators*, Complexity, 2021, 2021(1), 7979365.

[41] M. A. N. Oqielat, T. Eriqat, Z. Al-Zhour, O. Ogilat, A. El-Ajou and I. Hashim, *Construction of fractional series solutions to nonlinear fractional reaction-diffusion for bacteria growth model via Laplace residual power series method*, International Journal of Dynamics and Control, 2023, 11(2), 520–527.

[42] M. N. Oqielat, T. Eriqat, Z. Al-Zhour, A. El-Ajou and S. Momani, *Numerical solutions of time-fractional nonlinear water wave partial differential equation via Caputo fractional derivative: An effective analytical method and some applications*, Applied and Computational Mathematics, 2022, 21(2), 207–222.

[43] K. M. Owolabi and A. Atangana, *Chaotic behaviour in system of noninteger-order ordinary differential equations*, Chaos, Solitons and Fractals, 2018, 115, 362–370.

[44] P. Rahimkhani, Y. Ordokhani and E. Babolian, *Numerical solution of fractional pantograph differential equations by using generalized fractional-order Bernoulli wavelet*, Journal of Computational and Applied Mathematics, 2017, 309, 493–510.

[45] M. M. Al-Sawalha, A. Khan, O. Y. Ababneh and T. Botmart, *Fractional view analysis of Kersten-Krasil'shchik coupled KdV-mKdV systems with non-singular kernel derivatives*, AIMS Math., 2022, 7(10), 18334–18359.

[46] A. K. H. Sedeeg, *A coupling Elzaki transform and homotopy perturbation method for solving nonlinear fractional heat-like equations*, Am. J. Math. Comput. Model, 2016, 1, 15–20.

[47] R. Shah, Y. Alkhezi and K. Alhamad, *An analytical approach to solve the fractional Benney equation using the q-homotopy analysis transform method*, Symmetry, 2023, 15(3), 669.

[48] A. P. Shakir, T. A. Sulaiman, H. F. Ismael, N. A. Shah and S. M. Eldin, *Multiple fusion solutions and other waves behavior to the Broer-Kaup-Kupershmidt system*, Alexandria Engineering Journal, 2023, 74, 559–567.

[49] J. Shi, C. Liu and J. Liu, *Hypergraph-based model for modeling multi-agent q-learning dynamics in public goods games*, IEEE Transactions on Network Science and Engineering, 2024, 11(6), 6169–6179. DOI: 10.1109/TNSE.2024.3473941.

[50] Q. Shi, S. Wang and J. Yang, *Small parameters analysis applied to two potential issues for Maxwell-Schrödinger system*, Journal of Differential Equations, 2025, 424, 637–659. DOI: 10.1016/j.jde.2025.01.049.

[51] M. Suleman, T. Elzaki, Q. Wu, N. Anjum and J. U. Rahman, *New application of Elzaki projected differential transform method*, Journal of Computational and Theoretical Nanoscience, 2017, 14(1), 631–639.

[52] P. Sunthrayuth, A. M. Zidan, S. W. Yao and M. Inc, *The comparative study for solving fractional-order Fornberg-Whitham equation via ρ-Laplace transform*, Symmetry, 2021, 13(5), 784.

[53] H. Wang, Y. Hou, Y. He, C. Wen, B. Giron-Palomares, Y. Duan and Y. Wang, *A physical-constrained decomposition method of infrared thermography: Pseudo restored heat flux approach based on ensemble bayesian variance tensor fraction*, IEEE Transactions on Industrial Informatics, 2024, 20(3), 3413–3424. DOI: 10.1109/TII.2023.3293863.

[54] K. J. Wang and K. L. Wang, *Variational principles for fractal Whitham-Broer-Kaup equations in shallow water*, Fractals, 2021, 29(02), 2150028.

[55] Y. Xiao, Y. Yang, D. Ye and J. Zhang, *Quantitative Precision Second-Order Temporal Transformation Based Pose Control for Spacecraft Proximity Operations*, IEEE Transactions on Aerospace and Electronic Systems, 2024.

[56] H. Yang, Q. Feng, X. Wang, D. Urynbassarova and A. A. Teali, *Reduced biquaternion windowed linear canonical transform: Properties and applications*, Mathematics, 2024, 12(5), 743. DOI: 10.3390/math12050743.

[57] H. Yasmin, A. S. Alshehry, A. H. Ganie, A. Shafee and R. Shah, *Noise effect on soliton phenomena in fractional stochastic Kraenkel-Manna-Merle system arising in ferromagnetic materials*, Scientific Reports, 2024, 14(1), 1810.

[58] H. H. Zhang, Z. H. Fan and R. S. Chen, *Incomplete LU factorization preconditioner for the efficient solution of improved electric field integral equations*, in 2010 International Conference on Microwave and Millimeter Wave Technology, IEEE, 2010, 599–602.

[59] H. H. Zhang, Z. H. Fan and R. S. Chen, *Marching-on-in-degree solver of time-domain finite element-boundary integral method for transient electromagnetic analysis*, IEEE Transactions on Antennas and Propagation, 2013, 62(1), 319–326.

[60] H. H. Zhang, H. M. Yao and L. J. Jiang, *Novel time domain integral equation method hybridized with the macromodels of circuits*, in 2015 IEEE 24th Electrical Performance of Electronic Packaging and Systems (EPEPS), IEEE, 2015 135–138.

[61] S. Zhang, Y. Yang and H. Yang, *A meshless symplectic algorithm for nonlinear wave equation using highly accurate RBFs quasi-interpolation*, Applied Mathematics and Computation, 2017, 314, 110–120.

[62] Z. Zhang, M. Lin, D. Li, R. Wu, R. Lin and C. Yang, *An AUV-Enabled Dockable Platform for Long-Term Dynamic and Static Monitoring of Marine Pastures*, IEEE Journal of Oceanic Engineering, 2024.

[63] Y. Zhou and L. Peng, *On the time-fractional Navier-Stokes equations*, Computers and Mathematics with Applications, 2017, 73(6), 874–891.

Received January 2025; Accepted May 2025; Available online July 2025.